DALTON
FULL PAPER

Synthesis, X-ray crystal structures and properties of chromium complexes with semiquinonate and catecholate

Ho-Chol Chang,[a] Tomohiko Ishii,[b] Mitsuru Kondo[a] and Susumu Kitagawa *[a]

[a] *Department of Synthetic Chemistry and Biological Chemistry, Graduate School of Engineering, Kyoto University, Sakyo-ku, Kyoto 606-8501, Japan*
[b] *Department of Chemistry, Faculty of Science, Tokyo Metropolitan University, 1-1 Minamiohsawa, Hachioji-shi, Tokyo 192-0397, Japan*

Received 18th March 1999, Accepted 18th June 1999

The reaction of tris-tetrahalogeno-*o*-benzosemiquinonate chromium(III) complexes, $[Cr^{III}(X_4SQ)_3]$ (X = Cl **1a** or Br **1b**), with bis(cyclopentadienyl) cobalt $[Co^{II}Cp_2]$, tetramethyltetraselenafulvalene (TMTSF) and tetrakis(methylsulfanyl)tetrathiafulvalene (TMT-TTF) afforded four charge-transfer compounds, $[Co^{III}Cp_2][Cr^{III}(X_4SQ)_2(X_4Cat)]$ (X = Cl **2a** or Br **2b**), [TMT-TTF][$Cr^{III}(Br_4SQ)_2(Br_4Cat)$] **3b** and [TMTSF][$Cr^{III}(Br_4SQ)_2(Br_4Cat)$] **4b**, where Cat is catecholate. The paramagnetic $[Cr^{III}(X_4SQ)_2(X_4Cat)]^-$ complexes are commonly formed by cocrystallization with a diamagnetic $[Co^{III}Cp_2]^+$ cation for **2a**·C_6H_6 and **2b**, and paramagnetic TMT-TTF$^{\bullet+}$ and TMTSF$^{\bullet+}$ cations for **3b**·$C_6H_5CH_3$ and **4b**·$2CH_2Cl_2$, respectively. The one-electron reduced complexes, $[Cr^{III}(X_4SQ)_2(X_4Cat)]^-$, with two semiquinonate and one catecholate ligands were isolated and crystallographically characterized. The crystal structures of **2a**·C_6H_6 and **3b**·$C_6H_5CH_3$ consist of alternating stacks of cations and anionic complexes, which form one-dimensional column structures. On the other hand, the anionic complexes in **4b**·$2CH_2Cl_2$ form a hexagonal honeycomb network, whose cavities are occupied by the dimerized cation molecules. The temperature dependence of the magnetic susceptibilities reveals that all the $[Cr^{III}(X_4SQ)_2(X_4Cat)]^-$ complexes are in a ground state of $S = 1/2$, which results from the intramolecular antiferromagnetic interaction between $Cr^{III}(d^3)$ and two semiquinonates. In addition, **3b** and **4b** have a contribution of the paramagnetic TMT-TTF$^{\bullet+}$ (**3b**) and TMTSF$^{\bullet+}$ (**4b**) cations. In all compounds weak intermolecular magnetic interactions were recognized from the decrease of the $\chi_m T$ values at low temperature.

Introduction

Transition metal complexes with *o*-dioxolene ligands have been the subject of intensive research in the last few decades, because these afford a rich redox chemistry based on a variety of formal oxidation states not only for the metal center but also for the ligand moiety.[1] In particular, most intriguing are the valence tautomerism and mixed-charge ligands, attributable to the contiguity of the frontier orbital energy of the metal center and the ligands.[2] The latter series are related, in a sense, to a class of complexes with mixed-valence metal ions linked by a bridging ligand.

The homoleptic chromium(III) tris-semiquinonate complexes $[Cr^{III}(Cl_4SQ)_3]$ (Cl_4SQ = tetrachloro-*o*-benzosemiquinonate), $[Cr^{III}(phenSQ)_3]$ (phenSQ = 9,10-phenanthrenesemiquinonate) and $[Cr^{III}(3,5\text{-DTBSQ})_3]$ (3,5-DTBSQ = 3,5-di-*tert*-butyl-*o*-benzosemiquinonate) undergo both oxidation and reduction reactions to afford a seven-membered redox series, in which complexes having mixed-charge ligands are involved and where the oxidation state +3 for the chromium ion is retained (Scheme 1).[3] Among these, the structural and physical properties of $[Cr^{III}(Cl_4SQ)_3]$, $[Cr^{III}(3,5\text{-DTBSQ})_3]$ and $[Cr^{III}(Cat)_3]^{3-}$ (Cat = catecholate) have been characterized in detail,[3,4] whereas the intermediate species, generally written as $[Cr^{III}(SQ)_2(Cat)]^-$ and $[Cr^{III}(SQ)(Cat)_2]^{2-}$, have not been isolated and characterized X-ray crystallographically. Of the reported complexes, $[Cr^{III}(Cl_4SQ)_3]$ shows stepwise ligand-based reductions at 0.80, 0.42 and −0.02 V (*vs.* Ag–AgCl).[5] The electron withdrawing effect of the chlorine atoms makes the complex behave as a strong electron acceptor. Thus, it is possible to get the intermediate species by utilizing a reducing reagent. As the reducing reagent, we chose an organometallic donor $[Co^{II}Cp_2]$ and organic donors, tetrakis(methylsulfanyl)tetrathiafulvalene (TMT-TTF) and tetramethyltetraselenafulvalene (TMTSF),

$$[Cr^{III}(BQ)_3]^{3+} \rightleftharpoons [Cr^{III}(SQ)(BQ)_2]^{2+} \rightleftharpoons [Cr^{III}(SQ)_2(BQ)]^{+}$$
$$S = 3/2 \qquad S = 1 \qquad S = 1/2$$
$$\rightleftharpoons Cr^{III}(SQ)_3 \rightleftharpoons$$
$$S = 0$$
$$[Cr^{III}(SQ)_2(Cat)]^{-} \rightleftharpoons [Cr^{III}(SQ)(Cat)_2]^{2-} \rightleftharpoons [Cr^{III}(Cat)_3]^{3-}$$
$$S = 1/2 \qquad S = 1 \qquad S = 3/2$$

(BQ = Benzoquinone, SQ = Semiquinone and Cat = Catecholate

Scheme 1

which are well known to form a number of charge-transfer compounds.[6] In this paper we report the isolation of $[Cr^{III}(X_4SQ)_2(X_4Cat)]^-$ (X = Cl or Br) anionic complexes as charge-transfer compounds, their crystal structures and spectroscopic and magnetic properties.

Experimental

Materials

All chemicals were reagent grade. Hexacarbonylchromium $[Cr(CO)_6]$, tetrachloro-*o*-benzoquinone (Cl_4BQ), tetrabromo-*o*-benzoquinone (Br_4BQ), $[CoCp_2]$ and TMTSF were obtained from Aldrich, TMT-TTF from Tokyo Chemical Industry Co., Ltd. Syntheses of complexes **1a**, **1b**, **2a** and **2b** were carried out under a dry nitrogen atmosphere by use of standard Schlenk techniques with freshly distilled solvents.

Preparation of the compounds

$[Cr^{III}(Cl_4SQ)_3]\cdot 4C_6H_6$ 1a. A microcrystalline sample of

complex **1a** was prepared by the procedure described previously.[4a,5] The product was confirmed by elemental analysis. Found: C, 45.48; H, 2.05. $C_{42}H_{24}Cl_{12}CrO_6$ requires C, 45.77, H, 2.19%.

$[Cr^{III}(Br_4SQ)_3]\cdot 4C_6H_6$ 1b. The complex was prepared by a similar procedure to that for **1a**. A benzene solution (100 ml) containing $[Cr(CO)_6]$ (1.01 g, 4.59 mmol) and Br_4BQ (9.75 g, 23 mmol) was refluxed for 3 d under dry nitrogen. The suspension was filtered, and the powder obtained washed with benzene several times (7.03 g, 94%). The complex is soluble in carbon disulfide and dichloromethane. Found: C, 30.61; H, 1.47. $C_{42}H_{24}Br_{12}CrO_6$ requires C, 30.84; H, 1.48%. IR (KBr): 1475m, 1454s, 1433s, 1394w, 1329w, 1255m, 1178m, 1033w, 937m, 754m, 679s, 623w, 561w and 526w cm^{-1}. Absorption spectrum in CH_2Cl_2: λ_{max}/nm (ε/M^{-1} cm^{-1}) 1000 (1350 (sh)), 779 (6700), 540 (26900), 500 (16100 (sh)), 462 (9600 (sh)) and 317 (18000). Redox potential (CH_2Cl_2, 0.033 mM, 0.1 M (n-$C_4H_9)_4NClO_4$): $E_{1/2}$ 0.80, 0.40 and 0.14 V (*vs.* Ag–AgCl).

$[Co^{III}Cp_2][Cr^{III}(Cl_4SQ)_2(Cl_4Cat)]\cdot C_6H_6$ 2a·C_6H_6. The complex $[Co^{II}Cp_2]$ (29 mg, 0.153 mmol) was added to a CH_2Cl_2 suspension (100 ml) of **1a** (164 mg, 0.149 mmol) under dry nitrogen, turning from red-purple to blue-purple in a few minutes. The suspension was stirred for two days, then evaporated to a half volume. To the residue 100 ml of *n*-hexane were added. The solid product was collected by filtration and washed with small amounts of CH_2Cl_2 three times. Recrystallization from CH_2Cl_2–C_6H_6 gave dark purple single crystals with solvated benzene (123 mg, 83%). The compound is soluble in dichloromethane and acetone. Found: C, 38.43; H, 1.57. $C_{34}H_{16}Cl_{12}CoCrO_6$ requires C, 38.64; H, 1.53%. IR (KBr): 1476m, 1435m, 1416m, 1308s, 1248m, 1117s, 980m, 797s, 691m, 677m, 583w and 450s cm^{-1}.

$[Co^{III}Cp_2][Cr^{III}(Br_4SQ)_2(Br_4Cat)]$ 2b. To a 100 ml of CH_2Cl_2 suspension containing complex **1b** (154 mg, 0.0942 mmol) was added $[Co^{II}Cp_2]$ (18 mg, 0.0952 mmol) with stirring under dry nitrogen. After several hours the suspension gradually turned blue-purple. It was evaporated to half volume, and 100 ml *n*-hexane were added. The microcrystalline solid obtained was filtered off, washed with small amounts of CH_2Cl_2, and dried in vacuum (130 mg, 78%). The compound is soluble in dichloromethane and acetone. Found: C, 22.25; H, 1.19. $C_{28}H_{10}Br_{12}CoCrO_6$ requires C, 22.24; H, 0.67%. IR (KBr): 1487w, 1449m, 1412s, 1348w, 1312m, 1244s, 1211w, 1167s, 1107s, 1061m, 1009w, 934s, 860w, 752m, 727w, 700m, 623w, 560m and 500m cm^{-1}

[TMT-TTF]$[Cr^{III}(Br_4SQ)_2(Br_4Cat)]\cdot C_6H_5CH_3$ 3b·$C_6H_5CH_3$. Single crystals of complex **3b**·$C_6H_5CH_3$ were grown from a layered solution of a CS_2 solution of **1b** (0.369 mM) and a toluene solution of TMT-TTF (0.369 mM). Black cubic crystals were obtained after two weeks. They readily lose solvent in the air to give a desolvated compound which is insoluble in common organic solvents. Found: C, 18.95; H, 0.90. $C_{28}H_{12}Br_{12}CrO_6S_8$ requires C, 18.99; H, 0.68%. IR (KBr): 1472w, 1450w, 1418m, 1396s, 1315m, 1290m, 1250s, 1209m, 1159s, 1125s, 935s, 752m, 702s, 623w, 561w, 503w and 476w cm^{-1}

[TMTSF]$[Cr^{III}(Br_4SQ)_2(Br_4Cat)]\cdot 2CH_2Cl_2$ 4b·$2CH_2Cl_2$. Single crystals of complex **4b**·$2CH_2Cl_2$ were grown from a layered solution of a CS_2 solution of **1b** (0.58 mM) and a CH_2Cl_2 solution of TMTSF (0.58 mM). Dark green cubic crystals were obtained after 3 weeks which readily lose solvent in the air to give a desolvated compound as well as **3b**. The compound is insoluble in common organic solvents. Found: C, 18.95; H, 0.90. $C_{28}H_{12}Br_{12}CrO_6Se_4$ requires C, 18.99; H, 0.68%. IR (KBr): 1545m, 1474w, 1450m, 1427m, 1334m, 1282w, 1250m, 1209w, 1095s, 933s, 752m, 696s, 623w, 559w and 501w cm^{-1}.

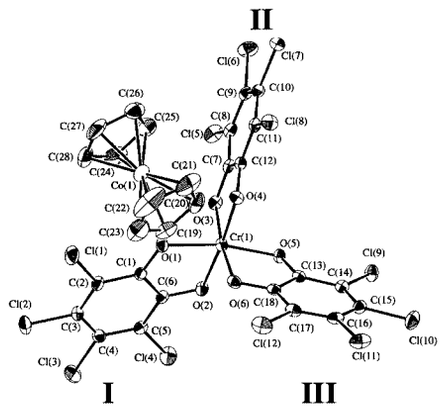

Fig. 1 An ORTEP drawing of complex **2a**·C_6H_6 (showing 20% anisotropic thermal ellipsoids). Crystallographically independent ligands are designated **I**, **II**, and **III**. The benzene molecule is omitted for clarity.

Physical measurements

For complexes **3b** and **4b** the desolvated samples were used for physical measurements. Infrared spectra for KBr pellets were recorded on a Hitachi I-5040 FT-IR spectrometer, absorption spectra on the KBr pellets on a Hitachi U-3500 spectrophotometer over the range from 300 to 3200 nm at room temperature. Electrochemical measurement of **1b** was carried out by a BAS CV-50W polarographic analyzer. A standard three-electrode system was used with a glassy carbon working electrode, platinum-wire counter electrode and Ag–AgCl electrode as reference. The EPR spectra were recorded on finely ground powders enclosed in a quartz tube at X-band frequency with a JEOL RE-3X spectrometer operating 9.0–9.5 GHz. The resonance frequency was measured on an Anritsu MF76A microwave frequency counter. Magnetic field was calibrated by an Echo Electronics EMF-2000AX NMR field meter. Magnetic susceptibilities were recorded over the temperature range from 1.9 to 300 K at 1 T with a superconducting quantum interference device (SQUID) susceptometer (Quantum Design, San Diego, CA) interfaced with a HP Vectra computer system. All values were corrected for diamagnetism calculated from Pascal's table.[7]

Crystallographic data collection and refinement of structures

Crystal structure determinations were carried out for complexes **2a**·C_6H_6, **3b**·$C_6H_5CH_3$ and **4b**·$2CH_2Cl_2$. All measurements were made on a Rigaku AFC7R diffractometer with graphite-monochromated Mo-Kα radiation and a rotating anode generator. All the crystal data are summarized in Table 1. The structures were solved by direct methods[8] and expanded using Fourier techniques.[9] All calculations were performed using TEXSAN.[10] All hydrogen atoms were placed in the idealized positions, but their parameters were not refined. The non-hydrogen atoms were refined anisotropically except for the toluene and dichloromethane molecules for **3b**·$C_6H_5CH_3$ and **4b**·$2CH_2Cl_2$, respectively. In **3b**·$C_6H_5CH_3$ disorder of the toluene molecule was found at the final stage, and thus its atom positions were isotropically refined under a rigid condition. In **4b**·$2CH_2Cl_2$ the positions of solvate atoms C(29), C(30) and Cl(1)–Cl(4) were determined from a Fourier map, but not refined.

CCDC reference number 186/1522.

See http://www.rsc.org/suppdata/dt/1999/2467/ for crystallographic files in .cif format.

Results and discussion

Molecular and crystal structures

Figs. 1–3 show ORTEP[11] drawings of complexes **2a**·C_6H_6, **3b**·$C_6H_5CH_3$ and **4b**·$2CH_2Cl_2$ with the atom numbering

Table 1 Crystallographic and refinement data for complexes **2a**·C_6H_6, **3b**·$C_6H_5CH_3$ and **4b**·$2CH_2Cl_2$

	2a·C_6H_6	**3b**·$C_6H_5CH_3$	**4b**·$2CH_2Cl_2$
Formula	$C_{34}H_{16}Cl_{12}CoCrO_6$	$C_{35}H_{20}Br_{12}CrO_6S_8$	$C_{30}H_{16}Br_{12}Cl_4CrO_6Se_4$
Formula weight	1056.86	1803.86	1940.95
Crystal system	Triclinic	Triclinic	Triclinic
Space group	$P\bar{1}$ (no. 2)	$P\bar{1}$ (no. 2)	$P\bar{1}$ (no. 2)
a/Å	13.961(3)	14.303(2)	13.523(6)
b/Å	14.297(3)	15.084(3)	16.177(8)
c/Å	10.950(4)	12.907(5)	12.406(7)
α/°	104.95(2)	109.62 (2)	111.43(4)
β/°	112.45(2)	99.31(2)	109.39(4)
γ/°	81.65(2)	91.86(2)	83.91(4)
V/Å^3	1948(1)	2577(1)	2382(2)
Z	2	2	2
μ(Mo-Kα)/cm^{-1}	15.71	99.19	136.531
T/K	296	296	296
Data measured	9316	10193	10417
Independent data	8945	9815	9953
No. data with $I > 3\sigma(I)$	4538	3232	3658
No. parameters	488	460	503
R_{int}	0.031	0.053	0.081
R, R'	0.042, 0.045	0.063, 0.064	0.057, 0.058

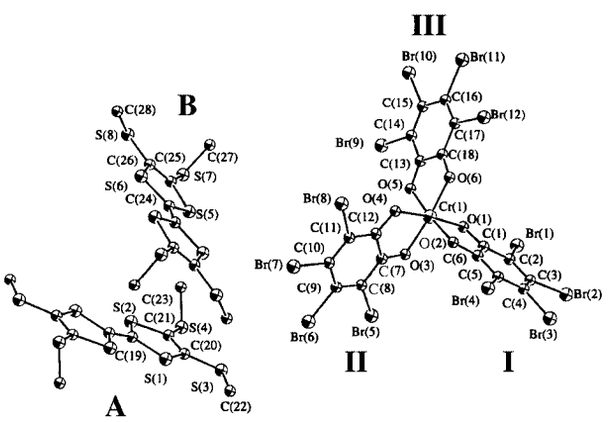

Fig. 2 An ORTEP drawing of complex **3b**·$C_6H_5CH_3$ with hydrogen atoms and solvent molecule omitted (showing 30% isotropic thermal ellipsoids). The TMT-TTF molecules **A** and **B** have their centroids coincident with crystallographic symmetry. Crystallographically independent ligands are designated **I**, **II**, and **III**.

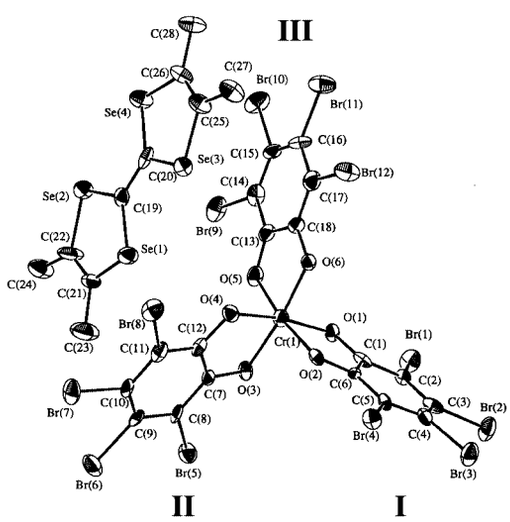

Fig. 3 An ORTEP drawing of complex **4b**·$2CH_2Cl_2$ with hydrogen atoms and solvent molecules omitted (showing 30% anisotropic thermal ellipsoids). Crystallographically independent ligands are designated **I**, **II**, and **III**.

schemes. The complexes **2a**·C_6H_6 and **4b**·$2CH_2Cl_2$ contain one crystallographically independent [$CoCp_2$] and TMTSF molecule, respectively, whereas **3b**·$C_6H_5CH_3$ has two crystallographically independent TMT-TTF molecules which are designated **A** and **B**. Each compound contains one crystallographically independent [$Cr(C_6O_2X_4)_3$] (X = Cl **2a** or Br **3b** and **4b**) complex where the three ligands are denoted **I**, **II** and **III**. Each compound is solvated, with benzene (**2a**), toluene (**3b**) and two dichloromethane (**4b**) molecules, respectively. Table 2 lists selected bond distances and angles of the compounds with their estimated deviations.

Cationic molecules. Complexes **2a**·C_6H_6 contains a [$CoCp_2$] complex with an eclipsed D_{5h} conformation. The bond distances between the cobalt atom and the carbon atoms fall in the range 1.981(9)–2.014(7) Å (av. 2.005(7) Å), which are shorter than that of cobaltocene (2.096(8) Å),[12a] but close to those of a typical [$Co^{III}Cp_2$]$^+$ cation,[12b] indicating the formation of [$Co^{III}Cp_2$]$^+$ cation.

The TMT-TTF and TMTSF molecules are almost planar except for the four terminal methylsulfanyl and methyl groups for **3b**·$C_6H_5CH_3$ and **4b**·$2CH_2Cl_2$, respectively. In Tables 3 and 4 their bond distances and angles are compared with the corresponding distances found in other compounds.[6c,13] The central C–C bond distances are most sensitive to the oxidation state of the molecules.[14] The values are 1.38(4) and 1.42(5) Å for TMT-TTF (**A**) and TMT-TTF (**B**) molecules, respectively, longer than those of neutral molecules and comparable to those of 1 : 1 charge-transfer compounds, [TMT-TTF]$^{\cdot+}$[$FeCl_4$]$^-$ and [TMT-TTF]$^{\cdot+}$[IBr_2]$^-$. These features indicate that all the TMT-TTF molecules in **3b**·$C_6H_5CH_3$ exist as a mono-cation form, TMT-TTF$^{\cdot+}$. A similar trend for TMTSF is recognized, leading to the formation of the mono-cation, TMTSF$^{\cdot+}$. The mono-cations were also confirmed by the disappearance of the C=C bond vibration modes of the neutral molecules, TMT-TTF^0 and TMTSF^0 (Experimental section).

Anionic chromium complexes. In complexes **2a**·C_6H_6, **3b**·$C_6H_5CH_3$ and **4b**·$2CH_2Cl_2$ the environments about the chromium ions are all distorted octahedral with six oxygen atoms from the three bidentate $C_6O_2X_4$ (X = Cl **2a** or Br **3b** and **4b**) ligands. The total oxidation numbers of the anionic complexes are responsible for the combination of semiquinonate and catecholate because of the inertness of the chromium center in the redox process.[3,15] In Table 5 the total averaged values of Cr–O and C–O bond distances and O–Cr–O angles are compared with those of tris(semiquinonate or catecholate) chromium complexes synthesized so far. It has been demonstrated that [$Cr^{III}(SQ)_3$], undergoes one-, two- and three-electron reduction

Table 2 Selected bond distances (Å) and angles (°) for complexes **2a**·C_6H_6, **3b**·$C_6H_5CH_3$ and **4b**·$2CH_2Cl_2$

2a·C_6H_6

$CoCp_2$

Co(1)–C(19)	2.008(7)	Co(1)–C(20)	2.010(7)
Co(1)–C(21)	2.006(7)	Co(1)–C(22)	2.014(7)
Co(1)–C(23)	2.011(7)	Co(1)–C(24)	1.981(9)
Co(1)–C(25)	1.998(8)	Co(1)–C(26)	2.012(7)
Co(1)–C(27)	2.006(6)	Co(1)–C(28)	2.000(7)

Ligand **I**

Cr(1)–O(1)	1.961(3)	C(1)–O(2)	1.949(3)
O(1)–C(1)	1.292(5)	O(2)–C(6)	1.291(5)
C(1)–C(2)	1.413(6)	C(1)–C(6)	1.425(6)
C(2)–C(3)	1.377(7)	C(3)–C(4)	1.405(7)
C(4)–C(5)	1.372(7)	C(5)–C(6)	1.403(6)
Cr(1)–O(1)–C(1)	112.6(3)	Cr(1)–O(2)–C(6)	113.1(3)
O(1)–Cr(1)–O(2)	81.9(1)		

Ligand **II**

Cr(1)–O(3)	1.937(3)	Cr(1)–O(4)	1.935(3)
O(3)–C(7)	1.296(5)	O(4)–C(12)	1.302(5)
C(7)–C(8)	1.408(6)	C(7)–C(12)	1.425(6)
C(8)–C(9)	1.363(7)	C(9)–C(10)	1.404(7)
C(10)–C(11)	1.376(6)	C(11)–C(12)	1.408(6)
Cr(1)–O(3)–C(7)	112.2(3)	Cr(1)–O(4)–C(12)	112.0(3)
O(3)–Cr(1)–O(4)	82.7(1)		

Ligand **III**

Cr(1)–O(5)	1.932(3)	Cr(1)–O(6)	1.933(3)
O(5)–C(13)	1.308(5)	O(6)–C(18)	1.314(5)
C(13)–C(14)	1.394(6)	C(13)–C(18)	1.420(6)
C(14)–C(15)	1.380(7)	C(15)–C(16)	1.400(7)
C(16)–C(17)	1.371(7)	C(17)–C(18)	1.389(6)
Cr(1)–O(5)–C(13)	112.03	Cr(1)–O(6)–C(18)	111.9(3)
O(5)–Cr(1)–O(6)	83.3(1)		

Intermolecular distances

Cl(2)···Cl(10)[1]	3.434(2)	Cl(3)···Cl(6)[2]	3.242(2)
Cl(3)···Cl(9)[3]	3.593(2)	Cl(4)···Cl(12)[4]	3.457(2)
Cl(6)···Cl(9)[5]	3.592(2)	Cl(6)···Cl(11)[6]	3.288(2)
Cl(8)···Cl(11)[7]	3.592(2)		

Symmetry codes: (1) $-x, -y-1, -z-1$; (2) $2x+2y+2z$; (3) $x+1, y, z+1$; (4) $-x, -y-1, -z$; (5) $-x-1, -y-1, -z-1$; (6) $x, y+1, z$; (7) $-x-1, -y, -z-1$.

3b·$C_6H_5CH_3$

TMT-TTF (A)

S(1)–C(19)	1.70(2)	S(1)–C(20)	1.72(2)
S(2)–C(19)	1.73(2)	S(2)–C(21)	1.74(3)
S(3)–C(20)	1.75(2)	S(3)–C(22)	1.78(2)
S(4)–C(21)	1.75(2)	S(4)–C(23)	1.84(2)
C(19)–C(19)[10]	1.38(4)	C(20)–C(21)	1.33(3)

TMT-TTF (B)

S(5)–C(24)	1.70(3)	S(5)–C(25)	1.76(3)
S(6)–C(24)	1.73(2)	S(6)–C(26)	1.68(3)
S(7)–C(25)	1.73(3)	S(7)–C(27)	1.73(6)
S(8)–C(26)	1.73(3)	S(8)–C(28)	1.82(3)
C(24)–C(24)[10]	1.42(5)	C(25)–C(26)	1.42(4)

Ligand **I**

Cr(1)–O(1)	1.92(1)	Cr(1)–O(2)	1.92(1)
O(1)–C(1)	1.34(2)	O(2)–C(6)	1.33(2)
C(1)–C(2)	1.41(3)	C(1)–C(6)	1.40(3)
C(2)–C(3)	1.40(3)	C(3)–C(4)	1.36(4)
C(4)–C(5)	1.40(3)	C(5)–C(6)	1.39(3)
Cr(1)–O(1)–C(1)	111(1)	Cr(1)–O(2)–C(6)	111(1)
O(1)–Cr(1)–O(2)	84.3(6)		

Ligand **II**

Cr(1)–O(3)	1.96(1)	Cr(1)–O(4)	1.96(1)
O(3)–C(7)	1.28(3)	O(4)–C(12)	1.27(3)
C(7)–C(8)	1.41(3)	C(7)–C(12)	1.42(3)
C(8)–C(9)	1.34(3)	C(9)–C(10)	1.43(3)
C(10)–C(11)	1.36(3)	C(11)–C(12)	1.44(3)
Cr(1)–O(3)–C(7)	112(1)	Cr(1)–O(4)–C(12)	111(1)
O(3)–Cr(1)–O(4)	82.3(5)		

Ligand **III**

Cr(1)–O(5)	1.98(1)	Cr(1)–O(6)	1.94(1)
O(5)–C(13)	1.27(3)	O(6)–C(18)	1.25(3)
C(13)–C(14)	1.42(3)	C(13)–C(18)	1.47(3)
C(14)–C(15)	1.37(3)	C(15)–C(16)	1.42(3)
C(16)–C(17)	1.39(4)	C(17)–C(18)	1.42(3)
Cr(1)–O(5)–C(13)	112(1)	Cr(1)–O(6)–C(18)	115(1)
O(5)–Cr(1)–O(6)	81.0(6)		

Intermolecular distances

Br(1)···S(2)[1]	3.741(6)	Br(7)···S(4)[3]	3.596(7)
Br(4)···S(5)[2]	3.698(6)	Br(12)···S(6)[2]	3.726(9)
Br(8)···S(8)[4]	3.634(8)	Br(2)···Br(8)[6]	3.789(3)
Br(2)···Br(5)[5]	3.508(3)	Br(5)···Br(11)[8]	3.629(4)
Br(2)···Br(11)[7]	3.824(5)	Br(8)···Br(10)[9]	3.659(5)
Br(6)···Br(11)[8]	3.704(4)		
S(3)···S(3)[2]	3.23(1)		

Symmetry codes: (1) $x, y, z-1$; (2) $-x-2, -y, -z-1$; (3) $-x-1, -y, -z-1$; (4) $x-1, y+1, z$; (5) $-x-2, -y, -z$; (6) $x+1, y, z$; (7) $-x-2, -y-1, -z$; (8) $x, y-1, z$; (9) $-x-1, -y-1, -z$; (10) $-x, -y, -z$.

4b·$2CH_2Cl_2$

TMTSF

SE(1)–C(19)	1.85(2)	Se(1)–C(21)	1.90(3)
Se(2)–C(19)	1.83(2)	Se(2)–C(22)	1.86(2)
Se(3)–C(20)	1.82(2)	Se(3)–C(25)	1.86(2)
Se(4)–C(20)	1.87(2)	Se(4)–C(26)	1.87(2)
C(19)–C(20)	1.43(3)	C(21)–C(22)	1.36(3)
C(25)–C(26)	1.34(3)	C(21)–C(23)	1.49(3)
C(22)–C(24)	1.49(3)	C(25)–C(27)	1.46(3)

Ligand **II**

Cr(1)–O(3)	1.96(1)	Cr(1)–O(4)	1.95(1)
O(3)–C(7)	1.27(2)	O(4)–C(12)	1.31(2)
C(7)–C(8)	1.41(3)	C(7)–C(12)	1.45(3)
C(8)–C(9)	1.36(3)	C(9)–C(10)	1.45(3)
C(10)–C(11)	1.38(3)	C(11)–C(12)	1.36(2)
Cr(1)–O(3)–C(7)	113(1)	Cr(1)–O(4)–C(12)	113(1)
O(3)–Cr(1)–O(4)	81.7(5)		

Table 2 (*Contd.*)

4b·2CH_2Cl_2

Ligand **I**				Ligand **III**			
Cr(1)–O(1)	1.91(1)	Cr(1)–O(2)	1.94(1)	Cr(1)–O(5)	1.93(1)	Cr(1)–O(6)	1.93(1)
O(1)–C(1)	1.31(2)	O(2)–C(6)	1.31(2)	O(5)–C(13)	1.29(2)	O(6)–C(18)	1.33(2)
C(1)–C(2)	1.40(3)	C(1)–C(6)	1.44(3)	C(13)–C(14)	1.41(3)	C(13)–C(18)	1.41(3)
C(2)–C(3)	1.37(3)	C(3)–C(4)	1.35(3)	C(14)–C(15)	1.39(3)	C(15)–C(16)	1.43(3)
C(4)–C(5)	1.45(3)	C(5)–C(6)	1.39(3)	C(16)–C(17)	1.41(3)	C(17)–C(18)	1.41(3)
Cr(1)–O(1)–C(1)	114(1)	Cr(1)–O(2)–C(6)	113(1)	Cr(1)–O(5)–C(13)	111(1)	Cr(1)–O(6)–C(18)	111(1)
O(1)–Cr(1)–O(2)	82.3(6)			O(5)–Cr(1)–O(6)	83.4(6)		
Intermolecular distances							
Br(2)···Se(2)	3.905(4)	Br(6)···Br(11)[4]	3.747(4)	Br(4)···Se(1)[1]	3.681(4)	Br(6)···Br(9)[5]	3.559(3)
Br(4)···Se(4)[2]	3.849(4)	Br(8)···Br(8)[6]	3.719(5)	Br(12)···Se(3)	3.813(4)	Br(7)···Br(9)[2]	3.778(3)
Br(2)···Br(5)[3]	3.633(4)	Br(9)···Br(11)[7]	3.805(4)	Br(4)···Br(12)[1]	3.542(4)	Br(8)···Br(10)[7]	3.573(3)
Br(5)···Br(11)[4]	3.782(4)	Se(2)···Se(3)[8]	3.752(4)	3.752(4)			
Se(1)···Se(4)[8]	3.697(4)						

Symmetry codes: (1) $-x, -y-2, -z$; (2) $x, y, z-1$; (3) $-x+1, -y-2, -z$; (4) $x-1, y, z-1$; (5) $-x+1, -y-2, -z+1$; (6) $-x, -y-1, z$; (7) $-x, -y-1, -z$; (8) $-x, -y-2, -z-1$.

Table 3 Comparison of intramolecular bond distances (Å) and estimated charge (Q) for TMT-TTF$^{\delta+}$ compounds and TMT-TTF (**A**) and (**B**) in **3b**·$C_6H_5CH_3$

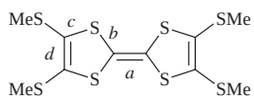

Compound	*a*	*b*	*c*	*d*	*Q*
TMT-TTF·TCNQ[a]	1.348(4)	1.748(3)	1.749(3)	1.337(3)	+0.4
[TMT-TTF][HCBD][b]	1.382(6)	1.724(4)	1.732(4)	1.364(5)	+0.4–0.6
TMT-TTF·$FeCl_4$[c]	1.380(9)	1.718(9)	1.736(8)	1.354(13)	+1
TMT-TTF·IBr_2[d]	1.392(13)	1.723(11)	1.741(10)	1.357(15)	+1
A	1.38(4)	1.72(2)	1.73(3)	1.33(3)	+1
B	1.42(5)	1.72(3)	1.72(3)	1.42(4)	+1

[a] From ref. 13(*a*). [b] From ref. 13(*b*), HCBD = hexacyanobutadiene. [c] From ref. 6(*c*). [d] From ref. 13(*c*).

Table 4 Comparison of intramolecular bond distances (Å) and estimated formal charge (Q) for TMTSF$^{\delta+}$ compounds and TMTSF in **4b**·2CH_2Cl_2

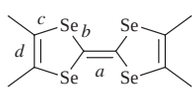

Compound	*a*	*b*	*c*	*d*	*Q*
TMTSF[a]	1.352(9)	1.892	1.906	1.315	0
$[TMTSF]_3[Pt(CN)_4]$[b]	1.352(11) 1.373(11)	1.878(8) 1.859(8)	1.901(8) 1.887(8)	1.323(12) 1.346(11)	+1/3
$[TMTSF]_2[PF_6]$[c]	1.369(14)	1.875(10)	1.893(10)	1.329(15)	+1/2
$[TMTSF]_3[W_6O_{19}]$[d]	1.36(4) 1.39(4)	1.86(3) 1.87(3)	1.88(3) 1.89(3)	1.33(4) 1.32(4)	+2/3
4b·2CH_2Cl_2	1.43(3)	1.84(2)	1.89(2)	1.35(3)	+1

[a] From ref. 13(*d*). [b] From ref. 13(*e*). [c] From ref. 12(*f*). [d] From ref. 12(*g*).

to provide the anionic complexes $[Cr^{III}(SQ)_{3-n}(Cat)_n]^{n-}$ ($n = 1$, 2 or 3),[3a] respectively. On the basis of the crystal structure of **2a**·C_6H_6, the counter cation is $[Co^{III}Cp_2]^+$, and consequently the chromium complex is $[Cr^{III}(Cl_4SQ)_2(Cl_4Cat)]^-$. Inspection of Table 5 reveals that the total averaged C–O distance and O–Cr–O angle of **2a**·C_6H_6 are larger than those of $[Cr^{III}(Cl_4SQ)_3]$, supporting that one of the three semiquinonate ligands is reduced to a catecholate. Complexes **3b**·$C_6H_5CH_3$ and **4b**·2CH_2Cl_2 show total averaged C–O bond distances and O–Cr–O angles similar to those of **2a**·C_6H_6, indicative of the formation of the $[Cr^{III}(Br_4SQ)_2(Br_4Cat)]^-$ complex. This is also substantiated by spectroscopic data shown below.

There have been many mixed-ligand complexes in the series $[M^{III}(N–N)(SQ)(Cat)]$ (N–N = bidentate nitrogen co-ligand, M = Fe or Co)[16] and $[V^{V}O(3,5\text{-DTBSQ})(3,5\text{-DTBCat})]_2$,[17] (3,5-DTBCat = 3,5-di-*tert*-butylcatecholate), which show crystallographically well distinguished mixed-charge states for the catecholate and the semiquinonate. On the other hand, two examples for homoleptic complexes, $[Ni^{II}(3,6\text{-DTBBQ})(3,6\text{-DTBSQ})_2]$[18] and $[Mn^{IV}(3,6\text{-DTBSQ})_2(3,6\text{-DTBCat})]$,[19] have been found. Of the three compounds obtained in this work, **3b**·$C_6H_5CH_3$ appears to show mixed-charge electronic structures between ligand **I** (catecholate) and **II** and **III** (semiquinonates). However distinction between the semiquinonate and catecholate for each compound is difficult because of crystallographic disorder.[16b,20] Clear assignments

Table 5 Intramolecular bond distances (Å) and angles (°) for tris(semiquinonate or catecholate) chromium complexes

Compound	Ligand	Cr–O			O–C			O–Cr–O	
			Intraligand average[a]	Total average[b]		Intraligand average[a]	Total average[b]		Total average[b]
$[Cr(Cl_4SQ)_3]$[c]				1.949(5)			1.280(1)		81.8(2)
$[Cr(3,5\text{-DTBSQ})_3]$[d]				1.932(5)			1.289(8)		81.4(2)
$[Cr(Cat)_3]^{3-}$[e]				1.986(3)			1.349(3)		83.6(1)
2a·C_6H_6	**I**	1.961(4), 1.949(3)	1.955(3)		1.292(5), 1.291(5)	1.292(2)		81.9(1)	
	II	1.937(4), 1.935(3)	1.936(3)		1.296(5), 1.302(5)	1.299(6)		82.7(1)	
	III	1.932(3) 1.933(3)	1.933(3)	1.941(3)	1.308(5), 1.314(5)	1.311(5)	1.301(5)	83.3(1)	82.6(1)
3b·$C_6H_5CH_3$	**I**	1.92(1), 1.92(1)	1.92(1)		1.34(2), 1.33(2)	1.34(2)		84.3(6)	
	II	1.96(1), 1.96(1)	1.95(2)		1.28(3), 1.27(3)	1.28(2)		82.3(5)	
	III	1.98(1), 1.94(1)	1.96(2)	1.95(2)	1.27(3), 1.25(3)	1.26(3)	1.29(2)	81.0(6)	82.4(6)
4b·$2CH_2Cl_2$	**I**	1.91(1), 1.94(1)	1.93(1)		1.31(2), 1.31(2)	1.31(2)		82.3(6)	
	II	1.96(1), 1.95(1)	1.96(1)		1.27(2), 1.31(2)	1.29(2)		81.7(5)	
	III	1.93(1), 1.93(1)	1.93(1)	1.94(1)	1.29(2), 1.33(2)	1.31(2)	1.30(2)	83.4(6)	82.5(6)

[a] Given by $\frac{1}{2}\Sigma_{i=1}^{2}(\text{Cr–O})_i$ and $\frac{1}{2}\Sigma_{i=1}^{2}(\text{C–O})_i$ for each ligand. [b] Given by $\frac{1}{6}\Sigma_{i=1}^{6}(\text{Cr–O})_i$, $\frac{1}{6}\Sigma_{i=1}^{6}(\text{C–O})_i$ and $\frac{1}{3}\Sigma_{i=1}^{3}(\text{O–Cr–O})_i$. [c] From ref. 4(*a*). [d] From ref. 3(*b*). [e] From ref. 4(*b*).

could be made by further quantitative structural analysis with greater precision. Nevertheless, the spectroscopic and magnetic susceptibility data support the localized catecholate and two semiquinonates in the anionic complexes (see below). Thus, hereafter, the anionic chromium complexes are written as $[Cr^{III}(X_4SQ)_2(X_4Cat)]^-$, without the assignment of the oxidation state to each ligand.

Crystal packing. The crystal packing of complex **2a**·C_6H_6 is illustrated in Fig. 4(*a*). A three-membered alternating stack of the $[Co^{III}Cp_2]^+$ cation (D), the $[Cr^{III}(Cl_4SQ)_2(Cl_4Cat)]^-$ complex (A) and the benzene (S) is recognized to form an infinite column ···DASDAS··· along the *b* axis. The mean separation between the least-squares planes is 3.538 (benzene···ligand **I**), 3.653 (ligand **I**···Cp) and 3.479 Å (benzene···Cp) with dihedral angles of 1.5, 18.55 and 17.72°, respectively. As shown in Fig. 4(*a*), the remaining ligands **II** and **III** are arranged on the same side of the column. This is because no steric factors operate in the arrangement, attributable to the large separation (14.3 Å) between the anionic complexes through the column. The columns are interlinked by the stack of the remaining ligands with mean interplanar distances of 3.507 (**II**···**II**) and 3.473 Å (**III**···**III**). The adjacent ligands stack in such a way that the C(9)–C(10) and C(9*)–C(10*) bonds overlap. A similar interaction is found in ligand **III** (C(15)–C(16)···C(15*)–C(16*)). These arrangements make a one-dimensional zigzag stacking structure of the anionic complexes ([··AA··] type) along the *b* axis, and are useful to interlink the nearest neighbor columns. The nearest Cr···Cr distance between the adjacent columns is 8.85 Å, while that in the column is 14.30 Å. In addition to the ligand stack, seven Cl···Cl contacts are found in the column and between the columns (Table 2), and consequently the anionic complexes form a two-dimensional network (Fig. 4(*b*)).

As shown in Fig. 5(*a*) the crystal structure of complex **3b**·$C_6H_5CH_3$ clearly shows a two-membered alternating stack of the TMT-TTF$^{\cdot+}$ cation and the $[Cr^{III}(Br_4SQ)_2(Br_4Cat)]^-$ complex along the [110] direction, typical of 1:1 charge-transfer compounds.[6f,21] The mean separation between the ligand **I** and the TMT-TTF$^{\cdot+}$ (**A**) and (**B**) cations is alternately 3.671 and 3.421 Å. The least-squares planes of the TMT-TTF$^{\cdot+}$ cations are tilted with respect to that of ligand **I** by 10.63 and 6.67°, respectively. The two TMT-TTF$^{\cdot+}$ cations are staggered to each other. In contrast with **2a**·C_6H_6, the remaining ligands (**II** and **III**) of the anionic complexes sit alternately on both sides of the column. This is associated with intermolecular steric interaction between the ligands (separation between ligands **I** = 6.8 Å).

There are three types of intermolecular interactions between cation···anion, cation···cation and anion···anion pairs. Fig. 5(*b*) shows five cation···anion pairs between the sulfur atoms of the TMT-TTF$^{\cdot+}$ cation and the bromine atoms of the $[Cr^{III}(Br_4SQ)_2(Br_4Cat)]^-$ complex. The S···Br contacts are in the range 3.596(7)–3.741(6) Å, which are all shorter than the sum (3.80 Å) of van der Waals radii of the two atoms. The cation···cation interaction of S(3)···S(3*) (3.23(1) Å), shorter than the sum (3.70 Å) of van der Waals radii, is found for the methylsulfanyl groups of the TMT-TTF$^{\cdot+}$ cations between the column. Six anion···anion interactions between the bromine atoms are also found. The distances for the contact interaction are summarized in Table 2.

As shown in Fig. 6(*a*) the anionic complexes in **4b**·$2CH_2Cl_2$ form an extended two-dimensional honeycomb layer in the *ac* plane, whose diagonal distance is approximately 12 Å. The layer is made up of mutual stacking arrangements of three ligands with mean separations 3.585 (**I**···**I**), 3.537 (**II**···**II**) and 3.566 Å (**III**···**III**). Among the stacks, ligands **II** and **III** form a one-dimensional zigzag stacking column ([··AA··] type), similar to that of **2a**·C_6H_6. The [··AA··] type column is interlinked by the additional stack of the ligand **I** to form a two-dimensional layer structure. An analogous honeycomb network has been found in two- or three-dimensional supramolecular host–guest systems.[22] In these honeycomb layer compounds the cation molecules play an important role in the determination of not only the interlayer separation but also the packing arrangement of the crystals. As shown in Fig. 6(*a*) each cavity in **4b**·$2CH_2Cl_2$ is occupied by two TMTSF$^{\cdot+}$ cations, where the cations can stack on top of each other but with a slight displacement along the long in-plane molecular axis. The short intermolecular contacts between the selenium atoms are observed between the molecules, namely 3.697(4) (Se(1)–Se(4*)) and 3.752(4) Å (Se(2)–Se(3*)). These distances are shorter than the sum of van der Waals radii (4.00 Å) of the two selenium atoms, showing a strong dimerization. The molecular plane of the dimer is perpendicularly directed to that of the layer. The arrangement of the dimers and the nearest neighboring $[Cr^{III}(Br_4SQ)_2(Br_4Cat)]^-$ complexes is shown in Fig. 6(*b*). The dimer is associated with four anionic complexes through Se···Br contacts in the range 3.681–3.905 Å, shorter than the sum (3.95 Å) of van der Waals radii of the two atoms. In addition, the TMTSF dimers stack with ligand **I** at a mean separation of 3.661 Å and dihedral angle of 4.38°. This arrangement makes an alternating stack of the TMTSF dimers and the $[Cr^{III}(Br_4SQ)_2(Br_4Cat)]^-$ complexes ([··DDAA··] type) through the [101] direction (Fig. 6(*a*)). Each dimer is separated by distances of 11 Å through the stack. With respect to the crystal stability, the TMTSF dimers seem to perform an important templating role for the construction of the anionic honeycomb layer. The stabilization is increased by the

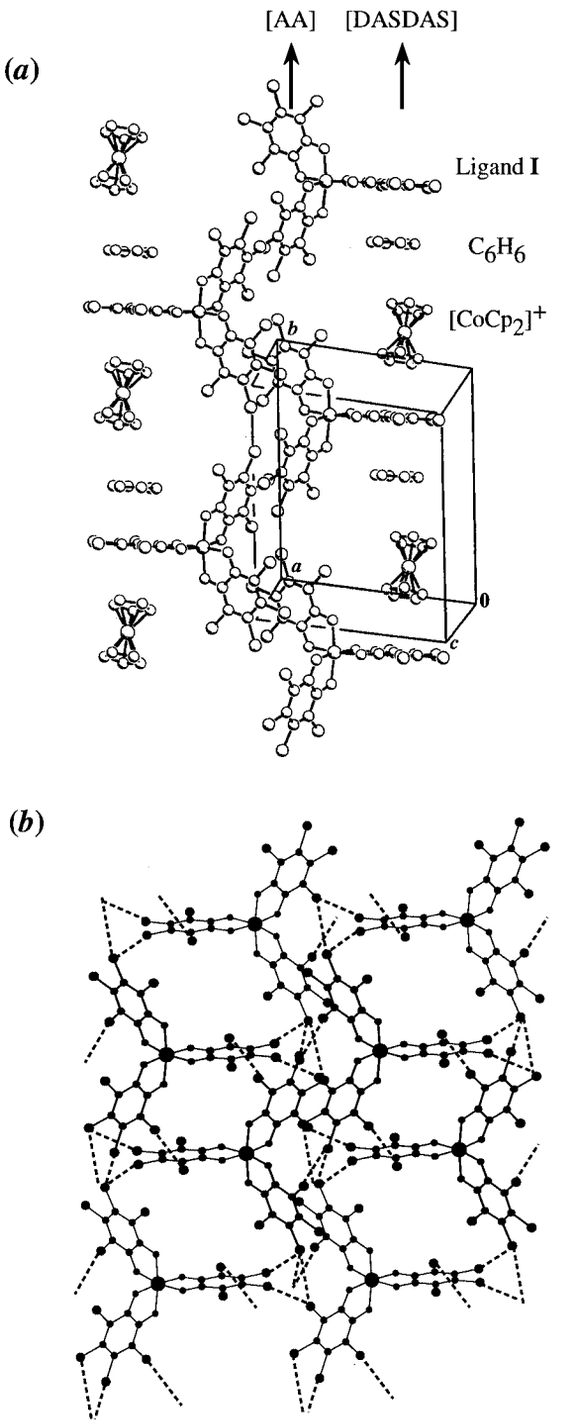

Fig. 4 (*a*) One-dimensional three-membered alternating stacking column of $[Co^{III}Cp_2]^+$, $[Cr^{III}(Cl_4SQ)_2(Cl_4Cat)]^-$ and benzene and (*b*) two-dimensional anion contacts through the intermolecular Cl···Cl interactions found in complex **2a**·C_6H_6.

intermolecular stacking arrangement enhanced by the planarity of the TMTSF molecule and the ligand.

Spectroscopic properties

Complexes **1a** and **1b** show an asymmetric IR band at ≈1460 cm^{-1}, characteristic of semiquinonate.[5] On the other hand, **2a**–**4b** show two kinds of bands, characteristic of semiquinonate and catecholate (≈1260 and ≈1480 cm^{-1}).[23] The frequencies are listed in the Experimental section.

Absorption spectral parameters for all the compounds are listed in Table 6. The absorption spectrum of **1b** is dominated by high-intensity charge-transfer bands mainly in the visible

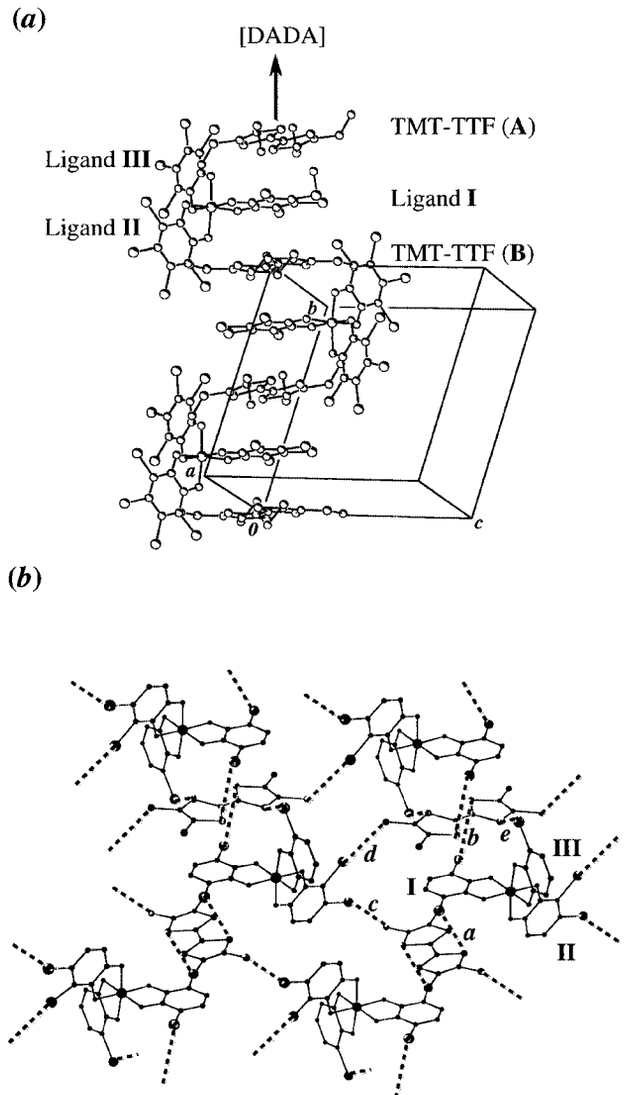

Fig. 5 (*a*) One-dimensional two-membered alternating stacking column of TMT-$TTF^{\bullet+}$ cations and $[Cr^{III}(Cl_4SQ)_2(Cl_4Cat)]^-$ complexes and (*b*) intra- and inter-column cation···anion contacts found in complex **3b**·$C_6H_5CH_3$: ***a*** [Br(1)···S(2)] = 3.741(6); ***b*** [Br(4)···S(5)] = 3.698(6); ***c*** [Br(7)···S(4)] = 3.596(7); ***d*** [Br(8)···S(8)] = 3.634(8); ***e*** [Br(12)···S(6)] = 3.726(9) Å. The methyl groups of TMT-TTF and the bromine atoms, which show no van der Waals contact with the sulfur atoms, are omitted for clarity.

region, and is in good agreement with that of **1a**, exhibiting similar electronic structures to each other.[5] Fig. 7 shows absorption spectra of **2a**·C_6H_6–**4b**. The spectral pattern of **2a**·C_6H_6 in the visible region is similar to that of $[Cr^{III}(3,5\text{-DTBSQ})_2(3,5\text{-DTBCat})]^-$ measured in solution.[3b] In addition, **2a**·C_6H_6 shows three characteristic absorptions at higher than 1400 nm. The maximum of the strongest absorption band is observed at 2546 nm. The corresponding band has been observed for a series of valence tautomeric complexes of Mn and Co.[16c,19,20,24] These bands are assigned to the intramolecular intervalence transition (IT) of catecholate to semiquinonate,[2a] indicating the presence of both ligands in the complex. Complex **2b** having the bromo-derivatives also shows a similar spectrum in the visible region and IT band at 2300 nm, indicating the similarity of its electronic structure with that of **2a**·C_6H_6. The IT bands are also observed for **3b** and **4b** (Fig. 7), indicating the presence of $[Cr^{III}(Br_4SQ)_2(Br_4Cat)]^-$. The maxima of the IT bands are observed at 2450 and 2400 nm for **3b** and **4b**, respectively. Comparison of the spectra of **3b** and **4b** with those of **2a** and **2b** leads to a conclusion that **2a**–**4b** have similar electronic structures, attributed to the $[Cr^{III}(X_4SQ)_2(X_4Cat)]^-$ complexes. The observed maxima of the IT bands are higher than those of

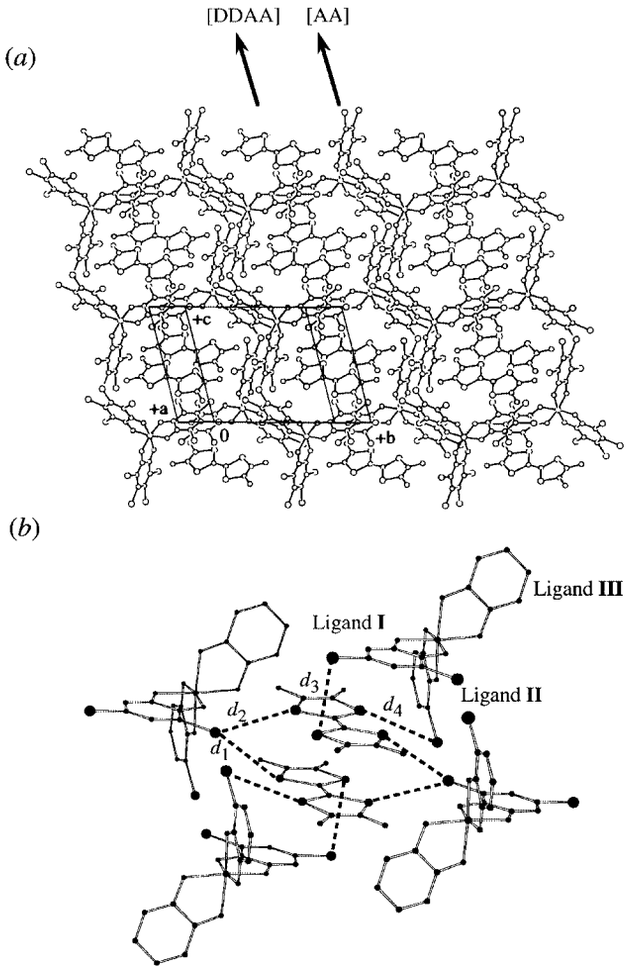

Fig. 6 (*a*) Honeycomb arrangement of the anionic complexes and (*b*) crystal packing structures of the TMTSF dimer and the nearest neighbor anion complexes with cation···anion contacts found in complex **4b**·2CH_2Cl_2; ***a*** [Se(1)···Br(4)] = 3.681(4); ***b*** [Se(4)···Br(4)] = 3.849(4); ***c*** [Se(2)···Br(2)] = 3.905(4); ***d*** [Se(3)···Br(12)] = 3.813(4) Å. The bromine atoms, which show no van der Waals contact with the selenium atoms, are omitted for clarity.

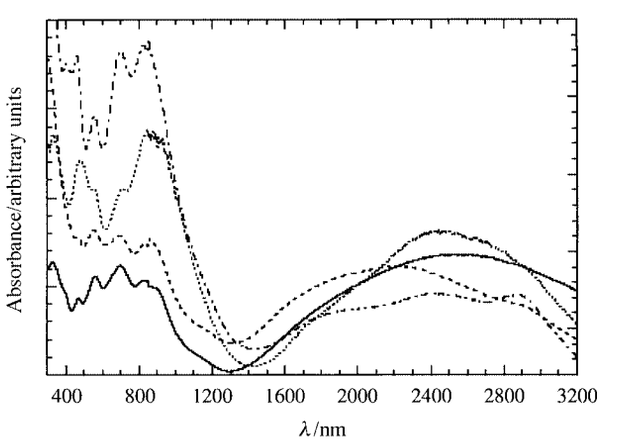

Fig. 7 Solid state absorption spectra (KBr) of complexes **2a**·C_6H_6 (—), **2b** (- - -), **3b** (– – –) and **4b** (–·–·).

manganese (2100 nm) complexes[19,20] while similar to those of cobalt (2400 nm) complexes.[2b,24]

Complexes **2a**–**4b** afford single EPR signals, independent of the temperature in the region of 77–300 K. The isotropic *g* values are summarized in Table 6. A solid sample of **2a**·C_6H_6 shows a signal at $g = 1.972$ with a linewidth of 15 G (77 K). The spectrum in a CH_2Cl_2–*n*-PrOH(1 : 1) glass at the same temperature consists of a signal at $g = 1.972$ with a linewidth of 5.6 G

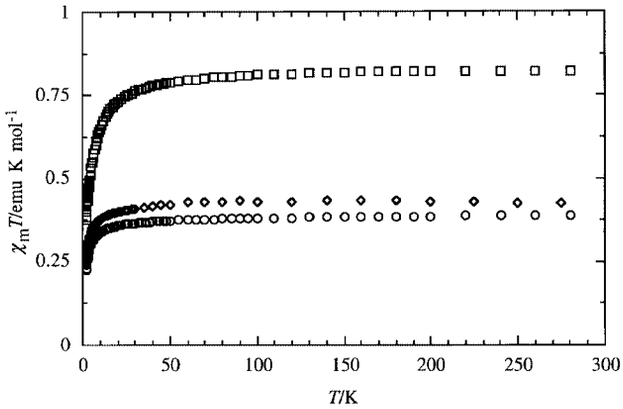

Fig. 8 Plots of the temperature dependence of $\chi_m T$ for complexes **2a**·C_6H_6 (○), **3b** (□) and **4b** (◇).

and hyperfine coupling (^{53}Cr, $I = 3/2$, 9.54% abundance) of 32.3 G. The *g* value is similar to that of the $[Cr^{III}(Cl_4SQ)_2(Cl_4Cat)]^-$ complex ($g = 1.9701$, $A(^{53}Cr) = 22.2$ G) measured in glass matrices, which has been electrochemically synthesized.[3a,4a] These results show that the unpaired electron in **2a**·C_6H_6 is on the chromium ion. Furthermore, the *g* values obtained for the solid and glass samples are identical, and the species in the solid and in solution have similar electronic structures. Similar results were obtained for **2b**.

Complexes **3b** and **4b** are expected to afford two types of EPR signals, attributable to the organic cations and the $[Cr^{III}(Br_4SQ)_2(Br_4Cat)]^-$ complex, when the two paramagnetic components are magnetically isolated. However, **3b** shows a single EPR signal at $g = 1.989$ from room to liquid nitrogen temperature, intermediate between those of the organic free radical ($g = 2.00$)[25] and the $[Cr^{III}(Br_4SQ)_2(Br_4Cat)]^-$ complex ($g = 1.968$ (**2b**)). This is associated with an exchange interaction between the two paramagnetic species in the solid state. On the other hand, the *g* value of **4b** is quite similar to that of **2b**, indicating that the unpaired electron is attributed to the $[Cr^{III}(Br_4SQ)_2(Br_4Cat)]^-$ complex. This is because the two $TMTSF^{\bullet+}$ cations form a dimer and their spins are antiferromagnetically coupled, which is also demonstrated by bulk magnetic susceptibility measurement.

Temperature-dependent magnetic susceptibilities

Complex 2a·C_6H_6. Fig. 8 shows the temperature dependence of $\chi_m T$ for complex **2a**·C_6H_6. At 300 K the value is estimated to be 0.392 emu K mol^{-1}, close to the theoretical value of 0.375 emu K mol^{-1}, expected for $S = 1/2$ ($g = 2.00$).[7] The anionic complex of **2a**·C_6H_6 contains a trivalent chromium ion with $S = 3/2$, two Cl_4SQ radicals with $S = 1/2$ and one nonmagnetic Cl_4Cat, namely $[Cr^{III}(Cl_4SQ)_2(Cl_4Cat)]^-$. Therefore, the observed unpaired electron is consistent with strong antiferromagnetic interactions between the $S = 3/2$ spin and two $S = 1/2$ spins on the semiquinonates.[1a,4c] In fact, the interaction is so strong that one can hardly detect a small amount of thermal population to the excited $S = 3/2$ state[4c] in this compound even at 300 K; this result is similar to those for the monosemiquinonate complexes $[Cr^{III}(tren)(3,6\text{-DTBSQ})][PF_6]_2$ (tren = tris(2-aminoethyl)amine)[26a] and $[Cr^{III}(CTH)(3,5\text{-DTBSQ})]_2Cl[PF_6]_3$ (CTH = *rac*-5,7,7,12,14,14-hexamethyl-1,4,8,11-tetraazacyclotetradecane),[26b] for which the lower limit of the isotropic coupling constant *J* is estimated to be larger than 350 cm^{-1} ($\boldsymbol{H} = 2J\cdot S_{Cr}\cdot S_{SQ}$). In the region of *ca.* 50–300 K the $\chi_m T$ value exhibits temperature-independent behavior, whereas below *ca.* 50 K, a rapid decrease is observed. Finally, the value decreases to 0.223 emu K mol^{-1} at 1.9 K. The decrease suggests intermolecular antiferromagnetic interactions between the neighboring $[Cr^{III}(Cl_4SQ)_2(Cl_4Cat)]^-$ complexes. These are attributable to the intermolecular Cl···Cl contacts between the adjacent anionic complexes (Fig. 4(*b*)). The contacts are

Table 6 Solid state absorption spectral parameters and isotropic g values for compounds **1a**–**4b**

Compound	λ/nm										g^a
1a[b]			1260	1040		776	537		465	415	
1b			1280	1060		785	545		465	415	
2a·C_6H_6	2900 (sh)	2546	1700 (sh)	930 (sh)	826	698	564		475		1.972
2b	2950 (sh)	2300	1700 (sh)	920 (sh)	834	698	562		470		1.968
3b	2950 (sh)	2450	1700 (sh)	930 (sh)	850	705	553	495 (sh)	477	400	1.989
4b	2900	2400	1900 (sh)	920 (sh)	820	700	560		465	400	1.968

[a] Measured on solid samples at 77 K. [b] From ref. 5.

shorter than the sum of van der Waals radii, and therefore could be a path for intermolecular magnetic interactions. On the other hand, intermolecular magnetic interactions in the *tert*-butyl-substituted complexes have not been observed[26a] due to the large *tert*-butyl groups, which hinder them. In conclusion, the $[Cr^{III}(Cl_4SQ)_2(Cl_4Cat)]^-$ complex is in the triplet state ($S = 1/2$) over the temperature range 50–300 K, and at < 50 K is in the singlet ground state ($S = 0$) due to the intermolecular antiferromagnetic interactions.

Complexes 3b and 4b. Temperature dependencies of $\chi_m T$ for complexes **3b** and **4b** are shown in Fig. 8. Both compounds consist of paramagnetic cations and $[Cr^{III}(Br_4SQ)_2(Br_4Cat)]^-$ complexes. If there is no magnetic interaction among them, the $\chi_m T$ value can be estimated to be 0.75 emu K mol^{-1} by assuming an isotropic g of 2.00; the observed value at 300 K is 0.847 emu K mol^{-1}. The large $\chi_m T$ value may be attributed to thermal population into the $S = 3/2$ excited state of the anionic complex. In the region 130–300 K, the $\chi_m T$ value obeys the Curie–Weiss law, that is $\chi_m = C/(T - \theta)$, with $\theta = -2.0$ K. At < 130 K the $\chi_m T$ value decreases to 0.377 emu K mol^{-1} at 2 K. This suggests a weak antiferromagnetic interaction between the TMT-TTF$^{\bullet+}$ cations and the $[Cr^{III}(Br_4SQ)_2(Br_4Cat)]^-$ complexes. In fact, there are many intermolecular S · · · Br contacts which are shorter than the sum of the van der Waals radii of the two atoms (Fig. 4(*b*) and Table 2) together with the anion · · · anion and cation · · · cation interactions. In addition the crystal structure of **3b**·$C_6H_5CH_3$ shows the intermolecular stacking structure of the TMT-TTF$^{\bullet+}$ cations and the $[Cr^{III}(Br_4SQ)_2(Br_4Cat)]^-$ complexes that could support such intermolecular magnetic interactions.

Complex **4b** shows $\chi_m T$ of 0.433 emu K mol^{-1} at 300 K, only 58% of the expected value for two moles of $S = 1/2$ spins. Inspection of the crystal structure indicates spin cancellation in the TMTSF dimers, and is consistent with the result of the EPR measurement. Therefore, the apparent magnetic susceptibility is attributed to the $[Cr^{III}(Br_4SQ)_2(Br_4Cat)]^-$ complexes. The $\chi_m T$ value shows temperature-independent behavior ($\theta = -0.1$ K) in the region 45–300 K, and at < 45 K decreases to 0.245 emu K mol^{-1} at 2 K, indicative of antiferromagnetic interaction. From the crystal structure, intra- and inter-layer magnetic interactions of the $[Cr^{III}(Br_4SQ)_2(Br_4Cat)]^-$ complexes are recognized. With regard to the intralayer magnetic interactions, the intermolecular stacks of the ligands are attributed to the magnetic interactions. On the other hand, the intermolecular Br · · · Br contacts between the anionic complexes of the neighboring layers lead to interlayer magnetic interactions.

Conclusion

In this work we have first isolated anionic chromium complexes with mixed-charge ligands, $[Cr^{III}(X_4SQ)_2(X_4Cat)]^-$, as charge-transfer compounds with organic and organometallic cations. The anionic complex contains semiquinonate (SQ) and catecholate (Cat), and shows a band in the near-infrared region characteristic of the intramolecular intervalence band between the two ligands. The crystal structures of the compounds are dependent on the donor molecules; **2a**·C_6H_6 and **3b**·$C_6H_5CH_3$ form an alternating stack of the cations and the $[Cr^{III}(X_4SQ)_2(X_4Cat)]^-$ complexes, whereas in **4b**·$2CH_2Cl_2$ the intermolecular stacking arrangement of the ligands results in the formation of a two-dimensional honeycomb layer, stabilized by the TMTSF dimers in the cavities.

Acknowledgements

The authors are grateful to Professor Cortlandt G. Pierpont, and acknowledge financial support by a Grant-in-Aid for Scientific Research (Priority Area No. 10149101) from The Ministry of Education, Science, Sports and Culture of Japan.

References

1 (*a*) C. G. Pierpont and C. W. Lange, *Prog. Inorg. Chem.*, 1994, **41**, 331; (*b*) C. G. Pierpont and R. M. Buchanan, *Coord. Chem. Rev.*, 1981, **38**, 45.
2 (*a*) D. M. Adams, L. Noodleman and D. N. Hendrickson, *Inorg. Chem.*, 1997, **36**, 3966; (*b*) O.-S. Jung and C. G. Pierpont, *J. Am. Chem. Soc.*, 1994, **116**, 2229; (*c*) C. Roux, D. M. Adams, J. P. Itié, A. Polian, D. N. Hendrickson and M. Verdaguer, *Inorg. Chem.*, 1996, **35**, 2846.
3 (*a*) H. H. Downs, R. M. Buchanan and C. G. Pierpont, *Inorg.Chem.*, 1979, **18**, 1736; (*b*) S. R. Sofen, D. C. Ware, S. R. Cooper and K. N. Raymond, *Inorg. Chem.*, 1979, **18**, 234.
4 (*a*) C. G. Pierpont and H. H. Downs, *J. Am. Chem. Soc.*, 1976, **98**, 4834; (*b*) K. N. Raymond, S. S. Isied, L. D. Brown, F. R. Fronczek and J. H. Nibert, *J. Am. Chem. Soc.*, 1976, **98**, 1767; (*c*) R. M. Buchanan, S. L. Kessel, H. H. Downs, C. G. Pierpont and D. N. Hendrickson, *J. Am. Chem. Soc.*, 1978, **100**, 7894; (*d*) R. M. Buchanan, H. H. Downs, W. B. Shorthill, C. G. Pierpont, S. L. Kessel and D. N. Hendrickson, *J. Am. Chem. Soc.*, 1978, **100**, 4318; (*e*) D. J. Gordon and R. F. Fenske, *Inorg. Chem.*, 1982, **21**, 2907.
5 C. G. Pierpont, H. H. Downs and T. G. Rukavina, *J. Am. Chem. Soc.*, 1974, **96**, 5573.
6 (*a*) G. Saito, T. Enoki, H. Inokuchi, H. Kumagai, C. Katayama and J. Tanaka, *Mol. Cryst. Liq. Cryst.*, 1985, **120**, 345; (*b*) K. Imaeda, T. Enoki, T. Mori, P. Wu, M. Kobayashi and H. Inokuchi, *Synth. Met.*, 1987, **19**, 721; (*c*) H. Endres, *Acta Crystallogr., Sect. C*, 1987, **43**, 439; (*d*) T. Enoki, J. Yamaura, N. Sugiyasu, K. Suzuki and G. Saito, *Mol. Cryst. Liq. Cryst.*, 1993, **233**, 325; (*e*) K. Bechgaard, C. S. Jacobsen, K. Mortensen, H. J. Pedersen and N. Thorup, *Solid State Commun.*, 1980, **33**, 1119; (*f*) A. E. Underhill, J. S. Tonge, P. I. Clemenson, H.-H. Wang and J. M. Williams, *Mol. Cryst. Liq. Cryst.*, 1985, **125**, 439; (*g*) S. Triki, L. Ouahab, J. Padiou and D. Grandjean, *J. Chem. Soc., Chem. Commun.*, 1989, 1068.
7 O. Kahn, *Molecular Magnetism*, VCH, New York, 1993.
8 SIR 92, A. Altomare, M. C. Burla, M. Camalli, M. Cascarano, C. Giacovazzo, A. Guagliardi and G. Pilidori, *J. Appl. Crystallogr.*, 1994, **27**, 435.
9 DIRDIF 94, P. T. Beurskens, G. Admiraal, G. Beurskens, W. P. Bosman, R. de Gelder, R. Israel and J. M. M. Smits, Technical Report of the Crystallography Laboratory, University of Nijmegen, 1994.
10 TEXSAN, Crystal Structure Analysis Package, Molecular Structure Corporation, The Woodlands, TX, 1985 and 1992.
11 C. K. Johnson, ORTEP II, Report ORNL-5138, Oak Ridge National Laboratory, Oak Ridge, TN, 1976.
12 (*a*) W. Bunder and E. Weiss, *J. Organomet. Chem.*, 1975, **92**, 65; (*b*) R. D. W. Kemmitt and D. R. Russell, *Comprehensive Organometallic Chemistry*, eds. G. A. Wilkinson, F. G. A. Stone and E. W. Abel, Pergamon, Oxford, 1982.
13 (*a*) T. Mori, P. Wu, K. Imaeda, T. Enoki and H. Inokuchi, *Synth. Met.*, 1987, **19**, 545; (*b*) C. Katayama, M. Honda, H. Kumagai,

K. Tanaka, G. Saito and H. Inokuchi, *Bull. Chem. Soc. Jpn.*, 1985, **58**, 2272; (*c*) K. Honda, M. Goto, M. Kurahashi, H. Anzai, M. Tokumoto and T. Ishiguro, *Bull. Chem. Soc. Jpn.*, 1988, **61**, 588; (*d*) T. J. Kistenmacher, T. J. Emge, P. Shu and D. O. Cowan, *Acta Crystallogr.*, *Sect. B*, 1979, **35**, 772; (*e*) L. Ouahab, J. Padiou, D. Grandjean, C. Garrigou-Lagrange, P. Delhaes and M. Bencharif, *J. Chem. Soc.*, *Chem. Commun.*, 1989, 1038; (*f*) N. Thorup, G. Rindorf and H. Soling, *Acta Crystallogr.*, *Sect. B*, 1981, **37**, 1236; (*g*) S. Triki, L. Ouahab, J. -F. Halet, O. Peña, J. Padiou, D. Grandjean, C. Garrigou-Lagrange and P. Delhaes, *J. Chem. Soc.*, *Dalton Trans.*, 1992, 1217.

14 P. Guionneau, C. J. Kepert, G. Bravic, D. Chasseau, M. R. Truter, M. Kurmoo and P. Day, *Synth. Met.*, 1997, **86**, 1973.

15 R. M. Buchanan, J. Claflin and C. G. Pierpont, *Inorg.Chem.*, 1983, **22**, 2552.

16 (*a*) R. M. Buchanan and C. G. Pierpont, *J. Am. Chem. Soc.*, 1980, **102**, 4951; (*b*) A. S. Attia, S. Bhattacharya and C. G. Pierpont, *Inorg. Chem.*, 1995, **34**, 4427; (*c*) O.-S. Jung, D. H. Jo, Y.-A. Lee, B. J. Conklin and C. G. Pierpont, *Inorg. Chem.*, 1997, **36**, 19; (*d*) O.-S. Jung and C. G. Pierpont, *Inorg. Chem.*, 1994, **33**, 2227.

17 M. E. Cass, D. L. Greene, R. M. Buchanan and C. G. Pierpont, *J. Am. Chem. Soc.*, 1983, **105**, 2680.

18 C. W. Lange and C. G. Pierpont, *Inorg. Chim. Acta*, 1997, **263**, 219.

19 A. S. Attia and C. G. Pierpont, *Inorg. Chem.*, 1998, **37**, 3051.

20 A. S. Attia and C. G. Pierpont, *Inorg. Chem.*, 1997, **36**, 6184; 1995, **34**, 1172.

21 C. Bellitto, M. Bonamico, V. Fares and P. Serino, *Inorg. Chem.*, 1996, **35**, 4070; L. J. Pace, A. Ulman and J. A. Ibers, *Inorg. Chem.*, 1982, **21**, 199; J. S. Kasper and L. V. Interrante, *Acta Crystallogr.*, *Sect. B*, 1976, **32**, 2914.

22 S. Decurtins, H. W. Schmalle, H. R. Oswald, A. Linden, J. Ensling, P. Gütlich and A. Hauser, *Inorg. Chim. Acta*, 1994, **216**, 65; H. Tamaki, Z. J. Zhong, N. Matsumoto, S. Kida, M. Koikawa, N. Achiwa, Y. Hashimoto and H. Okawa, *J. Am. Chem. Soc.*, 1992, **114**, 6974; C. J. Nuttall, C. Bellitto and P. Day, *J. Chem. Soc.*, *Chem. Commun.*, 1995, 1513.

23 M. W. Lynch, M. Valentine and D. N. Hendrickson, *J. Am. Chem. Soc.*, 1982, **104**, 6982; M. E. Cass, N. R. Gordon and C. G. Pierpont, *Inorg. Chem.*, 1986, **25**, 3962.

24 O.-S. Jung, D. W. Jo, Y.-A. Lee, H. K. Chae and Y. S. Sohn, *Bull. Chem. Soc. Jpn.*, 1996, **69**, 2211.

25 J. M. Williams, J. R. Ferraro, R. J. Thorn, K. D. Carlson, U. Geisen, H. H. Wang, A. M. Kini and M.-H. Whangbo, *Organic Superconductors* (*including Fullerenes*), Prentice Hall, Englewood Cliffs, NJ, 1992.

26 (*a*) D. E. Wheeler and J. K. McCusker, *Inorg. Chem.*, 1998, **37**, 2296; (*b*) C. Benelli, A. Dei, D. Gatteschi, H. U. Güdel and D. Pardi, *Inorg. Chem.*, 1989, **28**, 3089.

Paper 9/02162K